Hopping processes explain linear rise in temperature of thermal conductivity in thermoelectric clathrates with off-center guest atoms

Qing Xi,[1,2,3] Zhongwei Zhang,[1,2,3] Jie Chen,[1,2,3] Jun Zhou,[1,2,3,*] Tsuneyoshi Nakayama,[1,2,3,4,†] and Baowen Li[5,‡]

[1]*Center for Phononics and Thermal Energy Science, School of Physics Science and Engineering,*
Tongji University, 200092 Shanghai, People's Republic of China
[2]*China-EU Joint Center for Nanophononics, School of Physics Science and Engineering, Tongji University,*
200092 Shanghai, People's Republic of China
[3]*Shanghai Key Laboratory of Special Artificial Microstructure Materials and Technology,*
School of Physics Science and Engineering, Tongji University, 200092 Shanghai, People's Republic of China
[4]*Hokkaido University, 060-0826 Sapporo, Japan*
[5]*Department of Mechanical Engineering, University of Colorado, Boulder, Colorado 80309, USA*

Type-I clathrate compounds with off-center guest ions can be used to realize the concept of phonon-glass electron-crystal because they exhibit lattice thermal conductivities κ_L that are almost identical to those observed in network-forming glasses. This is in contrast with type-I clathrates with on-center guest ions, which show κ_L of conventional crystalline structures. Glasslike κ_L stems from the peculiar THz frequency dynamics in off-center type-I clathrates, in which there appear three kinds of modes classified as extended, weakly localized (WL) and strongly localized (SL) modes, as demonstrated by Liu *et al.* [Phys. Rev. B **93**, 214305 (2016)]. Our calculated results based on the hopping mechanism of SL modes via anharmonic interactions show fairly good agreement with the observed T-linear rise of κ_L above the plateau at a few tens Kelvin. We emphasize that both the magnitude and the temperature dependence are in accord with the experimental data of off-center type-I clathrates.

I. INTRODUCTION

Lattice thermal conductivity constitutes a key element to improve the efficiency of thermal-to-electrical conversion in thermoelectric (TE) devices as understood from the material's figure of merit describing the efficiency $Z = S^2\sigma/\kappa_{tot}$ (K^{-1}). The numerator contains the Seebeck coefficient $S(T)$ (V/K) and the electrical conductivity $\sigma(T)$ [1/(Ωm)], while the denominator $\kappa_{tot}(T)$ [W/(mK)] consists of the sum of electrical κ_{el} and lattice κ_L thermal conductivity. Hence, the high performance of thermoelectricity can be achieved for materials with the lowest possible thermal conductivity κ_{tot}, the highest possible electrical conductivity σ, and the highest possible Seebeck coefficient S. Provided that the Wiedemann-Franz law $\kappa_{el}(T) \propto \sigma(T)$ holds, κ_L becomes a crucial parameter to improve the performance of TE conversion. In this framework, Slack [1] has proposed the concept of a "phonon-glass electron-crystal". This has been one of the guiding principles for exploring high-performance TE materials [2,3].

Type-I clathrates with "off-center" guest ions, such as $R_8Ga_{16}Ge_{30}$ ($R =$ Ba,Sr,Eu) [4–9], $Ba_8Ga_{16}Sn_{30}$ [10,11], and $Sr_8Ga_{16}Si_{30-x}Ge_x$ [12], are particularly interesting in this respect since these systems exhibit lattice thermal conductivities that are almost identical to those of structural glasses, which consist of four specific regions characterized by (i) $T^{\sim 2}$ dependence below a few Kelvin, (ii) the plateau region between a few K and a few 10 K, (iii) the subsequent rise proportional to T, and (iv) its saturation above $T \sim 100$ K. These characteristics of κ_L exhibit a remarkable uniformity that

appears to be insensitive to chemical compositions, suggesting the existence of a unified mechanism [13]. However, this issue remains an open and challenging problem due to the difficulty to identify relevant entities or elements at the atomistic level caused by their complex microscopic structures. Surprisingly enough, though "off-center" clathrates are crystalline with regularly network structure, the temperature dependence as well as the magnitudes of their thermal conductivities are almost identical to those of structural glasses over the full temperature range. In contrast, type-I clathrates with "on-center" guest ions show conventional crystalline κ_L [2].

This paper is organized as follows. Section II surveys the characteristics of vibrational modes according to the results of the spectral density of states, eigenvalues, and their eigenvectors [14]. We claim in this section that the onset of the plateau is due to the delocalization-localization (weak localization) transition of acoustic modes. In addition, we point out that the temperature region showing the subsequent T-linear rise is associated with the energy range where strongly localized (SL) modes are fully excited. Section III describes the construction of the anharmonic interaction Hamiltonian between SL and extended modes. The second-quantized form of the anharmonic Hamiltonian is given in Sec. IV. In Sec. V, a theory is developed regarding the mechanism governing the T-linear rise of $\kappa_L(T)$ above a few 10 K. Excited modes in this temperature region are mostly SL modes satisfying the Ioffe-Regel condition, as is evident from the mode pattern obtained by large-scale numerical simulations [14]. These are hybridized modes between acoustic phonons associated with network cages and local vibrations of guest ions in cages. Based on this numerical evidence, we explain in a quantitative manner $\kappa_L(T)$ proportional to T by introducing the quantum-mechanical process of hopping of SL modes due to anharmonic interactions, first proposed for fracton

*zhoujunzhou@tongji.edu.cn
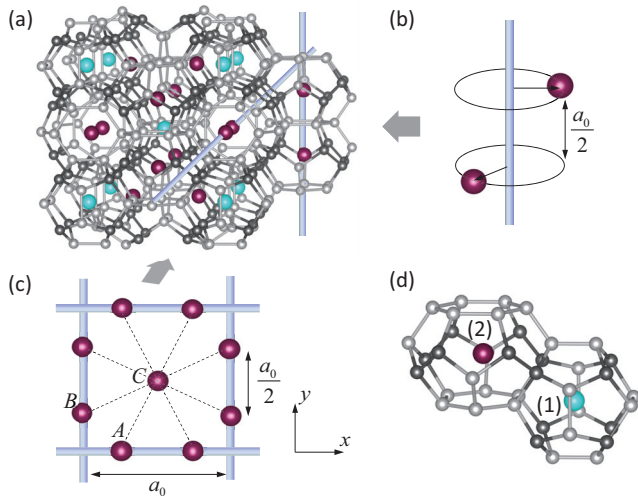†tnaka@eng.hokudai.ac.jp
‡baowen.li@colorado.edu

FIG. 1. (a) Illustration of type-I clathrate. The fourfold inversion axes are directed along the x, y, and z axes. Red and blue balls represent off-center guest ions in tetrakaidecahedron cages and centered guest ions in dodecahedron cages, respectively. (b) Two off-center guest ions along the y axis are depicted. (c) The configuration of eight-nearest-neighbor guest ions connected by an equilateral triangle. The sites A, B, and C in (c) are seated on the chains parallel to x, y, and z, respectively: $A = (a/4,0,a/4)$, $B = (0,a/4,3a/4)$, and $C = (a/2,a/2,a/2)$. (d) The molecular unit composed of a tetrakaidecahedron cage with off-center guest ion (2) at a $24k$ site and a smaller dodecahedral cage with guest ion (1) at a $2a$ site.

excitations [15]. Summary and conclusions are given in Sec. VI.

II. CHARACTERISTICS OF EXCITED PHONONS IN THE THZ FREQUENCY REGION

Type-I clathrates form a primitive cubic structure ($Pm\bar{3}n$) consisting of 6 tetrakaidecahedron (14-hedrons) and 2 dodecahedron (12-hedrons) per unit cell, in which the group-I or -II elements in the Periodic Table are encaged in the polyhedrons as guest ions. See Fig. 1. The THz frequency phonon dynamics of off-center type-I clathrates has been investigated in terms of large-scale numerical simulations. They have illustrated type-I $Ba_8Ga_{16}Sn_{30}$ (BGS) exhibiting glasslike $\kappa_L(T)$ as a prototype material with off-center guest ions, in which the guest ion Ba(2) in a tetrakaidecahedron cage has mass m, and the molecular unit composed of one tetrakaidecahedron and 1/3 dodecahedron has total mass M excluding the off-center guest ion. The coarse-grained picture, an operation of reducing the degrees of freedom of the original system, is valid for our purposes due to the following reasons. First of all, extended acoustic modes at THz frequencies play a dominant role in heat transport since optical modes concerning to the vibrations of cages themselves do not contribute to thermal conductivity. Second, the wavelength λ of phonons in the frequency regime $\nu \leqslant 2.5$ THz ($E \leqslant 10$ meV) becomes $\lambda \geqslant 1.6$ nm, which is larger than the size of a unit cell of $a_0 \simeq 1$ nm in type-I clathrates, as estimated from the relation $\lambda = \nu/\nu$ using the sound velocity $\nu \approx 4 \times 10^3$ m/s. These validate the coarse-
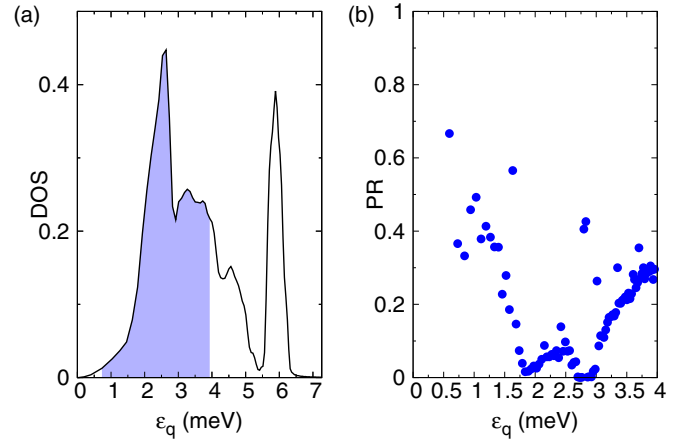

FIG. 2. (a). Calculated phonon density of states (DOS) of off-center type-I BGS for the system size of $99 \times 99 \times 99$ under a periodic boundary condition. (b) Calculated participation ratio $P(\varepsilon_q)$ defined in Eq. (1) as a function of eigenenergy ε_q in the energy range marking by the blue shadow in (a) for the system size of $20 \times 20 \times 20$ under a periodic boundary condition.

grained Hamiltonian for describing THz frequency dynamics rather than treating all microscopic constituents as equally relevant degrees of freedom.

Extremely large system sizes are required in computer simulations on disorder systems in order to distinguish localized modes from extended modes. However, the present status of first-principles calculations (FPC) is limited to insufficient system sizes for properly incorporating the disorder attributed to off-centeredness of guest atoms in off-center type-I clathrates consisting of a unit cell with "54" atoms. Thus, it is difficult not only to include realistic disorder reproducing glasslike thermal conductivities, but also to exclude the finite-size effect for propagating acoustic phonons. Liu *et al.* [14] have performed calculations for three-dimensional (3D) systems of $(20 \times 20 \times 20) \sim (100 \times 100 \times 100)$ molecular units, for which they have employed a powerful numerical method called the forced oscillator method [16,17]. They have also studied the localization nature of excited modes by taking the participation ratio (PR) as a criterion. The PR of a relevant mode $\{\varphi_\ell(\varepsilon_q); \ell = 1,2,\ldots,N\}$ belonging to the eigenenergy ε_q is defined by

$$P(\varepsilon_q) = \frac{\left(\sum_{\ell=1}^N |\varphi_\ell(\varepsilon_q)|^2\right)^2}{N \sum_{\ell=1}^N |\varphi_\ell(\varepsilon_q)|^4}, \qquad (1)$$

where ℓ denotes the ℓth molecular unit depicted in Fig. 1(d), and N is the total mode number. For extended modes, $P(\varepsilon_q)$ take values close to ≈ 0.6 when $\varepsilon_q \neq 0$, and $P(\varepsilon_q)$ becomes $\approx 1/N$ for SL modes [18]. Figure 2(a) is the calculated phonon density of states (DOS), and Fig. 2(b) shows the results of $P(\varepsilon_q)$ for the size of a $20 \times 20 \times 20$ lattice of off-center type-I BGS. It is remarkable that $P(\varepsilon_q)$ ranges from a value of SL modes $P(\varepsilon_q) \approx 0$ to extended modes of $P(\varepsilon_q) \approx 0.6$. We should emphasize that there appear three kinds of modes in the THz frequency region and below, classified into extended, weakly localized (WL), and SL modes. SL modes with PR values much smaller than unity are realized in the energy
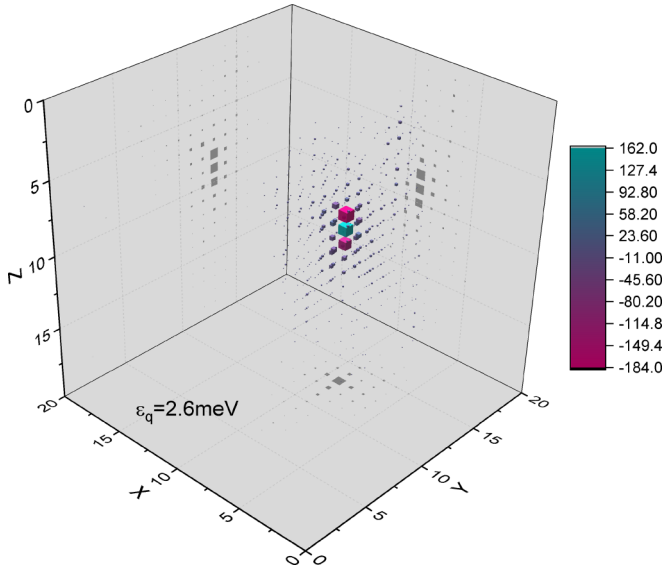
FIG. 3. The mode pattern of SL modes belonging to the eigenenergy $\varepsilon_q = 2.6$ meV. Both the color scale and the cubic size indicate the strength of amplitudes at each site. The mode pattern is obtained from the system size $20 \times 20 \times 20$ under a fixed boundary condition.

range from 2 to 3 meV as found from calculated mode patterns. Figure 3 depicts the mode patterns of a SL mode at $\varepsilon_q = 2.6$ meV.

The calculations of the PR for excited modes depicted in Fig. 2 have demonstrated that there is a delocalization-localization transition at a "finite" frequency ω_c distinguishing extended and WL modes with the nature of acoustic modes vibrating "in-phase" between guest ions and cages. Furthermore, it has been found [14] that WL modes convert to SL modes at higher frequencies with the nature of optical modes vibrating "out-of-phase" between guest ions and cages. In this aspect, we note that Nakayama [19] had demonstrated the clear existence of the transition from WL to SL modes for the quasi-one-dimensional (1D) coarse-grained model consisting of a host network and guest atoms connected by random springs. It was found [19] that WL modes vibrate in-phase between network atoms and guest atoms, while SL modes manifest optical modes vibrating out-of-phase. However, there are no extended modes due to the "quasi-1D" model. This manifests the Anderson weak-localization criteria where the critical frequency ω_c takes a finite value in 3D systems while it vanishes for 1D and 2D systems, suggesting there are no extended modes in 1D and 2D disordered systems. The quasi-1D model [19] should be thought of as the simplest theoretical model for cage-guest systems with broad implications for the dynamics of those systems.

The observed delocalization-localization transition at $\varepsilon_q \approx 1.3$ meV is in agreement with the observed onset temperature of the plateau of κ_L in BGS at $T_P \approx 1.3$ meV/$3.84k_B \approx 3.9$ K as estimated from Wien's displacement law for lattice thermal conductivities. Due to the weak localization of acoustic modes, the contribution of extended phonons "saturates" at T_P for off-center type-I BGS. We note here that the random orientation of guest ions in cages plays a crucial role in the localization.
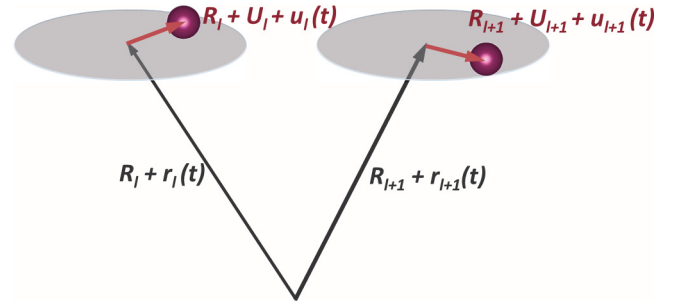

FIG. 4. The definition of the position vectors: $\boldsymbol{R}_\ell + \boldsymbol{r}_\ell(t)$ is the position vector of the ℓth molecular unit at time t, where $\boldsymbol{R}_\ell$ is the equilibrium position of the ℓth cage center, and the vector $\boldsymbol{r}_\ell(t)$ represents a small displacement from $\boldsymbol{R}_\ell$ at time t. The position vector of the guest ion(2) is defined by the vector $\boldsymbol{R}_\ell + \boldsymbol{U}_\ell + \boldsymbol{u}_\ell(t)$, where $\boldsymbol{U}_\ell$ is the equilibrium position of guest ion(2) from $\boldsymbol{R}_\ell$, and $\boldsymbol{u}_\ell(t)$ is a small displacement from $\boldsymbol{R}_\ell + \boldsymbol{U}_\ell$.

With increasing temperature further above a few 10 K, κ_L shows a linear rise in temperature [2]. These types of anomalous thermal conductivities have been clearly observed in off-center type-I clathrates [4,5,7,8,10–12]. SL modes are fully excited above the temperature $T \simeq 10$ K ≈ 3 meV/$3.84k_B$ from Wien's displacement law. This indicates that the T-linear rise can be attributed to the excitations of SL modes. In the following sections, we present a theoretical interpretation of the underlying mechanism of the linear rise on temperature above the plateau region for κ_L.

III. COARSE-GRAINED HAMILTONIAN FOR TYPE-I OFF-CENTER CLATHRATES

A. Harmonic Hamiltonian

The Hamiltonian for off-center type-I clathrates under a coarse-grained picture consists of the kinetic energy of networked cages K_C and off-center guest ions in cages K_G in addition to the potential energy of the cage-cage interaction V_{CC} and the cage-guest interaction V_{CG}. This is expressed by

$$H_0 = K_C + K_G + V_{CC} + V_{CG}. \tag{2}$$

The explicit form of the total kinetic energy is given by the sum of K_C and K_G such as

$$K = \frac{1}{2} \sum_\ell [M\dot{\boldsymbol{r}}_\ell(t)^2 + m\dot{\boldsymbol{u}}_\ell(t)^2], \tag{3}$$

where m and M are masses of the guest ion in a tetrakaidecahedron cage and the remaining molecular unit, respectively. The vectors $\boldsymbol{r}_\ell(t)$ and $\boldsymbol{u}_\ell(t)$ represent small displacements of cage and guest ions from their equilibrium positions, $\boldsymbol{R}_\ell$ and $\boldsymbol{R}_\ell + \boldsymbol{U}_\ell$, at the site ℓ as depicted in Fig. 4. Note here that guest ions take random orientation $\boldsymbol{U}_\ell(\phi_\ell)$ in tetrakaidecahedron cages.

The molecular unit composed of a tetrakaidecahedron and a dodecahedron is elastically connected with neighboring ones by the force constants $f_\parallel, f_\perp$. These are related to the sound velocities of longitudinal ($\mu = \parallel$) and transverse ($\mu = \perp$) acoustic modes via the relation $v_\mu = a[f_\mu/(m + M)]^{1/2}$ with $a = a_0/2$, where a_0 is the lattice spacing of the primitive cubic structure ($Pm\bar{3}n$) of type-I clathrates. Thus, we can estimate

the force constants $f_\parallel, f_\perp$ from the observed data of sound velocities. Note here that six molecular units are included in the unit cell in type-I clathrates. In terms of these quantities, the potential energy of network cages becomes

$$V_{CC} = \sum_{\ell' > \ell, \mu} \frac{f_{\ell, \ell', \mu}}{2} [r_{\ell, \mu}(t) - r_{\ell', \mu}(t)]^2, \quad (4)$$

where $\mu = \parallel, \perp, \perp'$. Hereafter, we keep up to the nearest-neighbor coupling ($\ell' = \ell + 1$) between molecular units, which are denoted by $f_\parallel, f_\perp$, and $f_{\perp'}$. The effect of randomly orientated guest ions is included in the following cage-guest interaction Hamiltonian.

The Hamiltonian should satisfy the symmetry of infinitesimal translation invariance as a whole, i.e., $r_\ell = u_\ell = \delta a$, which guarantees acoustic phonons as the Nambu-Goldstone boson with the eigenfrequency $\omega_k \to 0$ for $k \to 0$. This symmetry principle also holds for the potential of cage-guest interaction. Hence, the potential function for the cage-guest interaction V_{CG} should be given by relative coordinates between the cage and the guest ion of $w_\ell(t) = u_\ell(t) - r_\ell(t)$, which is expressed by

$$V_{CG} = \sum_{\ell, m = in, out} \frac{\xi_m}{2} w_{\ell, m}^2(t), \quad (5)$$

where ξ_m represents the force constants between the cage and the guest ion depending on in-plane (parallel) or out-of-plane motion (perpendicular) to the hexagonal face in the tetrakaidecahedron cage. The guest ions execute in-plane vibration parallel to the x-y plane in addition to out-of-plane motions [10] because of the anisotropic shape of tetrakaidecahedron cages, which distinguishes the vibrations of off-center guest ion(2) in the plane parallel and perpendicular to the hexagonal face of the cage. Mori *et al.* [20] observed by means of THz time-domain spectroscopy that the lowest-lying peak of off-center BGS at 0.71 THz splits into double peaks, $\omega_0^\phi/2\pi = 0.5$ THz and $\omega_0^r/2\pi = 0.72$ THz, for off-center type-I BGS below $T \simeq 100$ K. These spectra should be assigned to the libration and stretching modes of Ba(2) associated with ξ_ϕ and ξ_r. The peak around 1.35 THz is assigned as the out-of-plane motion of Ba(2) to the hexagonal faces of a tetrakaidecahedron, which should be concerned with ξ_θ. The Raman spectra of off-center $Sr_8Ga_{16}Ge_{30}$ (SGG) have shown the A_{1g} stretching mode as 48 cm^{-1}, and for off-center $Eu_8Ga_{16}Ge_{30}$ (EGG) as 36 cm^{-1} at 2 K [21]. Using these data, we can estimate the force constants via the relation $\xi_{r,(\phi,\theta)} = m' \omega_{r,(\phi,\theta)}^2$, where m' is the reduced mass defined by $1/m' = 1/M + 1/m$.

By taking account of this aspect, the quasiharmonic Hamiltonian valid at $T \lesssim 100$ K, attributed to coupled vibrations between cages and guest atoms, can be expressed in vector form as

$$V_{CG} = \frac{1}{2} \sum_\ell \xi_r (\hat{U}_\ell \cdot w_{\parallel, \ell})^2 + \frac{1}{2} \sum_\ell \xi_\phi (\hat{U}_\ell \times w_{\parallel, \ell})^2$$
$$+ \frac{1}{2} \sum_\ell \xi_\theta (w \perp, \ell)^2, \quad (6)$$

where $\hat{U}_\ell = (\hat{U}_\ell^x, \hat{U}_\ell^y)$ is the unit vector for the vector U_ℓ. $\{\phi_\ell\}$ and $\{\theta_\ell\}$ represent the azimuthal and the polar angle in

spherical coordinates. The effect of a "random" orientation of guest ions $\{\phi_\ell\}$ induced by off-centeredness is involved in $\{U_\ell\}$. The relation between off-centeredness and disorder in Eq. (6) is described in detail in the supplemental material [22].

B. Anharmonic coupling between acoustic phonons and SL modes

When acoustic modes (LA and TA) are propagating along networked cages, the cages are distorted and these change the states of guest ions, which are realized via the change of the force constants ξ_r and ξ_ϕ in Eq. (6). The in-plane (stretching and libration) modes are sensitive to temperature/pressure compared with out-of-plane modes as shown in the optic spectroscopy data below $T \simeq 100$ K [20,21]. Thus, the anharmonic effect between acoustic modes and in-plane modes in the first and the second terms in Eq. (6) becomes relevant in comparison with the third term. The expansions of ξ_r and ξ_ϕ with respect to the strain tensor $e_{\alpha\beta}$ for $\alpha, \beta = x, y, z$ provide

$$\xi_{r,(\phi)} = \xi_{r,(\phi)}^{(0)} + \sum_{\alpha=x,y,z} D_{r,(\phi)} e_{\alpha\alpha} + \sum_{\substack{\alpha,\beta=x,y,z \\ \alpha \neq \beta}} S_{r,(\phi)} e_{\alpha\beta} + \cdots.$$

$$(7)$$

Here the coefficients are defined by $D_{r,(\phi)} = \partial \xi_{r,(\phi)} / \partial e_{\alpha\alpha}$ and $S_{r,(\phi)} = \partial \xi_{r,(\phi)} / \partial e_{\alpha\beta(\alpha \neq \beta)}$, where $e_{\alpha\beta} = 1/2(\partial u_\alpha / \partial x_\beta + \partial u_\beta / \partial x_\alpha)$ is the component of the strain tensor. It should be noted that $e_{\alpha\alpha}$ expresses the compression or expansion, and $e_{\alpha\beta(\alpha \neq \beta)}$ expresses the shear distortion. The expansion in Eq. (7) leads to the following anharmonic interaction, expressed in vector form as

$$V_{CG}' = \frac{1}{2} \sum_{\ell, \alpha \neq \beta} (D_r e_{\alpha\alpha} + S_r e_{\alpha\beta})(\hat{U}_\ell \cdot w_{\parallel, \ell})^2$$
$$+ \frac{1}{2} \sum_{\ell, \alpha \neq \beta} (D_\phi e_{\alpha\alpha} + S_\phi e_{\alpha\beta})(\hat{U}_\ell \times w_{\parallel, \ell})^2. \quad (8)$$

Here we note that Eq. (8) satisfies the condition of infinitesimal translational invariance as a whole; $V_{CG}' \to 0$ under the long-wavelength limit $k_\mu \to 0$. We emphasize again that Eq. (8) is valid at temperatures $T \lesssim 100$ K where the guest atoms execute coupled vibrations with cages [20,21], while at $T \gtrsim 100$ K, $\kappa_L(T)$ saturates without exhibiting the appreciable T dependence, where guest atoms behave like rattlers in cages termed by the "rattling" motion, where the concept of vibrational modes is invalid [20,21].

IV. THE SECOND-QUANTIZED FORM OF THE INTERACTION HAMILTONIAN

A. Acoustic phonons resulting from networked cages

Provided that extended acoustic phonons with wavelengths λ much larger than the lattice spacing a_0 propagate through networked cages, the molecular units and guest ions vibrate "in phase." The displacement at site ℓ is expressed by the sum of plane waves as given by

$$r_\ell(t) = \sum_{k_\mu} \sqrt{\frac{\hbar}{2\rho \omega_{k_\mu}}} \hat{e}_{k_\mu} (\phi_{k_\mu}(R_\ell) b_{k_\mu}^\dagger(t) + H.c.). \quad (9)$$

Here the symbols $b_{\boldsymbol{k}_\mu}^\dagger$ ($b_{\boldsymbol{k}_\mu}$) express the creation (annihilation) operator for an acoustic phonon of the mode ($\boldsymbol{k}_\mu$) with $\mu = \parallel$, $\perp$, which represent longitudinal and transverse modes, respectively. The vector $\boldsymbol{R}_\ell$ expresses the equilibrium position of the ℓth molecular unit as depicted in Fig. 4, and H.c. denotes the Hermitian conjugate. The mass density is defined as $\rho = 6(m + M)/a_0^3$ with the size of the unit cell of a_0 since six molecular units are involved in the unit cell of type-I clathrates. See Sec. I in the supplemental material [22] for details on the definitions employed in this paper.

The function $\phi_{\boldsymbol{k}_\mu}(\boldsymbol{R}_\ell)$ in Eq. (9) takes the form

$$\phi_{\boldsymbol{k}_\mu}(\boldsymbol{R}_\ell) = \sqrt{\frac{1}{V}} e^{i\boldsymbol{k}_\mu \cdot \boldsymbol{R}_\ell}. \tag{10}$$

The normalization condition for $\phi_{\boldsymbol{k}_\mu}(\boldsymbol{R}_\ell)$ is given by

$$\int \left| \phi_{\boldsymbol{k}_\mu}(\boldsymbol{R}_\ell) \right|^2 d\boldsymbol{R}_\ell = 1. \tag{11}$$

B. SL modes due to guest ions

Figure 3 provides the mode belonging to the eigenenergy $\varepsilon_q = 2.6$ meV obtained for the system size $20 \times 20 \times 20$. This mode pattern indicates that the localization length L_λ is comparable with the wavelength $2\pi/k_\lambda$, i.e., localized within several molecular units, manifesting the Ioffe-Regel condition of strong localization. On the basis of these numerical findings, we can express the form of SL modes in terms of the relative coordinate $\boldsymbol{w}_\ell(t) = \boldsymbol{u}_l(t) - \boldsymbol{r}_l(t)$ as

$$\boldsymbol{w}_\ell(t) = \sum_\lambda \sqrt{\frac{\hbar}{2m'\omega_\lambda}} \hat{\boldsymbol{e}}_\lambda (\psi_\lambda(\boldsymbol{R}_\ell)c_\lambda^\dagger(t) + \text{H.c.}). \tag{12}$$

Here the mass m' is the reduced mass defined by $1/m' = 1/M + 1/m$, where M is the mass of the molecular unit given in Fig. 1, much larger than the mass of the guest ion m, e.g., $M = 6.01m$ for off-center type-I BGS. The symbol $c_\lambda^\dagger$ (c_λ) represents the creation (annihilation) operator for the localized mode λ. We put forward the ansatz for the amplitude $\psi_\lambda(\boldsymbol{R}_\ell)$ of the form

$$\psi_\lambda(\boldsymbol{R}_\ell) = A \cos[\boldsymbol{k}_\lambda \cdot (\boldsymbol{R}_\ell - \boldsymbol{R}_\lambda)] e^{-|\boldsymbol{R}_\ell - \boldsymbol{R}_\lambda|/L_\lambda}, \tag{13}$$

where $\boldsymbol{R}_\lambda$ represents the center of the SL mode λ. This wave function has vanishing group velocities v_g characterizing localized modes.

The prefactor A in Eq. (13) can be determined from the normalization condition of

$$\sum_\ell | \psi_\lambda(\boldsymbol{R}_\ell) |^2 = \frac{1}{\Omega} \int d\boldsymbol{R}_\ell | \psi_\lambda(\boldsymbol{R}_\ell) |^2 = 1, \tag{14}$$

where $\Omega = V/N$ is the volume of the molecular unit depicted in Fig. 1(d). This yields, by combining with the Ioffe-Regel condition,

$$A \cong \sqrt{\frac{2\Omega}{\pi L_\lambda^3}}. \tag{15}$$

The above has been obtained by using the formula $\cos^2(\boldsymbol{k} \cdot \boldsymbol{R}) = [\cos(2\boldsymbol{k} \cdot \boldsymbol{R}) + 1]/2$. According to the Ioffe-Regel condition $k \approx 2\pi/L_\lambda$, the first term in the integral

becomes negligible compared with the second term since the first term yields a rapidly oscillating function in the integrand. This leads to Eq. (15). Thus, the normalized wave function of the SL mode λ becomes

$$\psi_\lambda(\boldsymbol{R}_\ell) = \sqrt{\frac{2\Omega}{\pi L_\lambda^3}} \cos[\boldsymbol{k}_\lambda \cdot (\boldsymbol{R}_\ell - \boldsymbol{R}_\lambda)] e^{-|\boldsymbol{R}_\ell - \boldsymbol{R}_\lambda|/L_\lambda}. \tag{16}$$

C. Anharmonic Hamiltonian between SL and extended modes

We consider here the effect of incoming extended acoustic phonons with the polarization vector $\hat{\boldsymbol{e}}_{\boldsymbol{k}_\mu}$ to SL modes with the polarization vectors $\hat{\boldsymbol{e}}_{\lambda'}$ and $\hat{\boldsymbol{e}}_{\lambda''}$. These are included in Eq. (8) as the scalar product $(\hat{\boldsymbol{e}}_{\lambda'} \cdot \hat{\boldsymbol{U}}_\ell)(\hat{\boldsymbol{e}}_{\lambda''} \cdot \hat{\boldsymbol{U}}_\ell)$ and the product $(\hat{\boldsymbol{e}}_{\lambda'} \times \hat{\boldsymbol{U}}_\ell) \cdot (\hat{\boldsymbol{e}}_{\lambda''} \times \hat{\boldsymbol{U}}_\ell)$. At first, we fix the direction of the wave vector of incoming extended phonons $\boldsymbol{k}_\mu$, and later we include the contributions from three components of the wave vector $\boldsymbol{k}_\mu$. We should note that the deformation (normal or shear strain) of cages resulting from incoming acoustic phonons occurs in every direction of the polarization vector of SL modes, which provides both the interaction between the same polarization and different polarizations of SL modes, as shown below.

The second-quantized anharmonic Hamiltonian is obtained by substituting Eqs. (9) and (12) into Eq. (8) by using the relations given in Sec. II in the supplemental material [22]. The product of the field operators $b_{\boldsymbol{k}_\mu} c_{\lambda'} c_{\lambda''}$ consists of eight terms. The two involving the combinations $b_{\boldsymbol{k}_\mu}^\dagger c_{\lambda'}^\dagger c_{\lambda''}^\dagger$ and $b_{\boldsymbol{k}_\mu} c_{\lambda'} c_{\lambda''}$ are irrelevant to the hopping processes because they do not conserve the total energy. Furthermore, the other two terms $b_{\boldsymbol{k}_\mu}^\dagger c_{\lambda'} c_{\lambda''}$ and $b_{\boldsymbol{k}_\mu} c_{\lambda'}^\dagger c_{\lambda''}^\dagger$ do not contribute to the scattering processes since the energies of extended modes are smaller than those of SL modes. Hence, the relevant second-quantized anharmonic Hamiltonian for the process on extended $+$ SL $\rightarrow$ SL is given by

$$\begin{aligned} H'_{\text{CG}} = &\sum_{\boldsymbol{k}_\mu, \lambda', \lambda''} \left(A_{\boldsymbol{k}_\mu, \lambda', \lambda''} b_{\boldsymbol{k}_\mu} c_{\lambda'} c_{\lambda''}^\dagger + \text{H.c.} \right) \\ &+ \sum_{\boldsymbol{k}_\mu, \lambda''', \lambda''''} \left(B_{\boldsymbol{k}_\mu, \lambda''', \lambda''''} b_{\boldsymbol{k}_\mu} c_{\lambda'''} c_{\lambda''''}^\dagger + \text{H.c.} \right) \\ &+ \sum_{\boldsymbol{k}_\mu, \lambda', \lambda'''} \left(C_{\boldsymbol{k}_\mu, \lambda', \lambda'''} b_{\boldsymbol{k}_\mu} c_{\lambda'} c_{\lambda'''}^\dagger + \text{H.c.} \right), \end{aligned} \tag{17}$$

where $A_{\boldsymbol{k}_\mu, \lambda', \lambda''}$ is associated with the interaction between the modes with the x polarization, $B_{\boldsymbol{k}_\mu, \lambda''', \lambda''''}$ corresponds to the interaction between the y polarization, and $C_{\boldsymbol{k}_\mu, \lambda', \lambda'''}$ corresponds to the interaction between two different polarizations. See Fig. 5.

By taking the unit vectors $\hat{x}, \hat{y}, \hat{z}$ the same as the directions of the polarizations $\hat{\boldsymbol{e}}_\parallel, \hat{\boldsymbol{e}}_\perp, \hat{\boldsymbol{e}}_{\perp'}$ of extended acoustic modes, we have

$$\begin{aligned} &A_{\boldsymbol{k}_\mu, \lambda', \lambda''} \\ &= -\frac{1}{4} \sum_l i \sqrt{\frac{\hbar}{2\rho\omega_{\boldsymbol{k}_\mu}}} \sqrt{\frac{\hbar}{2m'\omega_{\lambda'}}} \sqrt{\frac{\hbar}{2m'\omega_{\lambda''}}} \\ &\quad \times \phi_{\boldsymbol{k}_\mu} \psi_{\lambda'} \psi_{\lambda''}[(D_r + D_\phi)k_\parallel \delta_{\mu,\parallel} + (S_r + S_\phi)k_\perp \delta_{\mu,\perp}], \end{aligned} \tag{18}$$
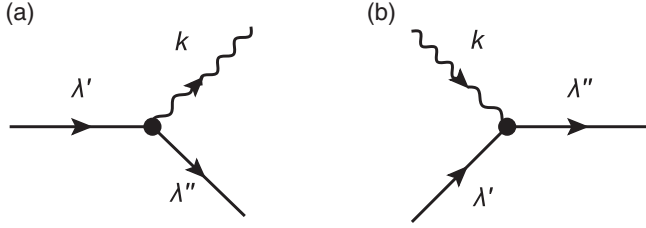
FIG. 5. The diagrams showing the hopping process for SL modes arising from anharmonic interaction between SL modes and extended modes: (a) SL $\rightarrow$ extended $+$ SL and (b) extended $+$ SL $\rightarrow$ SL. The solid lines denote the SL mode and the wavy lines the extended mode.

and the term on $B_{\boldsymbol{k}_\mu,\lambda''',\lambda''''}$ becomes the same as $A_{\boldsymbol{k}_\mu,\lambda',\lambda''}$ by setting $(\lambda',\lambda'' \longrightarrow \lambda''',\lambda'''')$. The last one should be

$$
\begin{aligned}
&C_{\boldsymbol{k}_\mu,\lambda',\lambda'''} \\
&= -\frac{1}{\pi}\sum_l i\sqrt{\frac{\hbar}{2\rho\omega_{\boldsymbol{k}_\mu}}}\sqrt{\frac{\hbar}{2m'\omega_{\lambda'}}}\sqrt{\frac{\hbar}{2m'\omega_{\lambda'''}}} \\
&\quad\times \phi_{\boldsymbol{k}_\mu}\psi_{\lambda'}\psi_{\lambda'''}[(D_r - D_\phi)k_\|\delta_{\mu,\|} + (S_r - S_\phi)k_\perp\delta_{\mu,\perp}].
\end{aligned}
\tag{19}
$$

The squared quantity on Eq. (18) is given by

$$
\begin{aligned}
A_{\boldsymbol{k}_\mu,\lambda',\lambda''}^2 = {} &\frac{CI_1^2}{VL_{\lambda'}^3 L_{\lambda''}^3}\frac{1}{\omega_{\boldsymbol{k}_\mu}\omega_{\lambda'}\omega_{\lambda''}} \\
&\times [(D_r + D_\phi)k_\|\delta_{\mu,\|} + (S_r + S_\phi)k_\perp\delta_{\mu,\perp}]^2,
\end{aligned}
\tag{20}
$$

where the coefficient C is defined as

$$
C = \frac{\hbar^3\Omega^2}{2^5\rho m'^2}.
\tag{21}
$$

The expression of $B_{\boldsymbol{k}_\mu,\lambda''',\lambda''''}^2$ takes the same form as $A_{\boldsymbol{k}_\mu,\lambda',\lambda''}^2$ since they both correspond to the interaction between SL modes with the same polarization, while $C_{\boldsymbol{k}_\mu,\lambda',\lambda'''}^2$ corresponding to the interaction between different polarizations has an additional factor $(4/\pi)^2$ and $[(D_r - D_\phi)k_\|\delta_{\mu,\|} + (S_r - S_\phi)k_\perp\delta_{\mu,\perp}]^2$.

V. HOPPING PROCESS

A. Relaxation time of SL modes

This subsection gives the formula for the relaxation time of a SL mode due to the scattering process extended $+$ SL $\rightarrow$ SL (hopping process) together with its reverse process shown in Fig. 5 by applying the Fermi golden rule. To obtain the total transition rate of the SL mode in λ', we have to incorporate all four processes for each polarization as given below. These provide the decay of the Bose-Einstein distribution function $n_{\lambda'}$ for the occupied state λ',

$$
\begin{aligned}
\frac{dn_{\lambda'}}{dt} = {} &\frac{2\pi}{\hbar^2}\sum_{\boldsymbol{k}_\mu,\lambda''}\left|A_{\boldsymbol{k}_\mu,\lambda',\lambda''}\right|^2\big[n_{\lambda''}\big(1+n_{\boldsymbol{k}_\mu}\big)(1+n_{\lambda'}) \\
&- n_{\boldsymbol{k}_\mu}n_{\lambda'}(1+n_{\lambda''})\big]\delta(\omega_{\lambda''} - \omega_{\lambda'} - \omega_{\boldsymbol{k}_\mu}) \\
&+ \left|A_{\boldsymbol{k}_\mu,\lambda'',\lambda'}\right|^2\big[n_{\boldsymbol{k}_\mu}n_{\lambda''}(1+n_{\lambda'}) - n_{\lambda'}\big(1+n_{\boldsymbol{k}_\mu}\big) \\
&\times (1+n_{\lambda''})\big]\delta(\omega_{\lambda'} - \omega_{\lambda''} - \omega_{\boldsymbol{k}_\mu}) \\
&+ \big[A_{\boldsymbol{k}_\mu,\lambda',\lambda''} \longrightarrow C_{\boldsymbol{k}_\mu,\lambda',\lambda'''},\lambda'' \longrightarrow \lambda'''\big].
\end{aligned}
\tag{22}
$$

We consider, at first, the decay due to the hopping process between the same polarization, i.e., the contribution from the first two terms of Eq. (22). By separating the distribution function into two parts, $n = n^{(0)} + n^{(1)}$, where $n^{(0)}$ is the Bose-Einstein distribution function in an equilibrium state and $n^{(1)}$ is its deviation due to the scattering processes, and by employing the relaxation-time approximation, $dn_{\lambda'}^{(1)}/dt = -n_{\lambda'}^{(1)}/\tau_{\lambda'}$, we have the inverse of relaxation time from Eq. (22) for the same polarization process,

$$
\begin{aligned}
\frac{1}{\tau_{\lambda'}^{\mathrm{same}}} \cong {} &\frac{2\pi}{\hbar^2}\frac{CI_1^2}{VL^6}\sum_{\boldsymbol{k}_\mu,\lambda''}\frac{1}{\omega_{\boldsymbol{k}_\mu}\omega_{\lambda'}\omega_{\lambda''}} \\
&\times [(D_r + D_\phi)k_\|\delta_{\mu,\|} + (S_r + S_\phi)k_\perp\delta_{\mu,\perp}]^2 \\
&\times \big[\delta(\omega_{\lambda''} - \omega_{\lambda'} - \omega_{\boldsymbol{k}_\mu})\big(n_{\boldsymbol{k}_\mu}^{(0)} - n_{\lambda''}^{(0)}\big) \\
&+ \delta(\omega_{\lambda'} - \omega_{\lambda''} - \omega_{\boldsymbol{k}_\mu})\big(1 + n_{\boldsymbol{k}_\mu}^{(0)} + n_{\lambda''}^{(0)}\big)\big],
\end{aligned}
\tag{23}
$$

where the explicit form of the summation I_1 arising from the overlapping of wave functions $\psi_{\lambda'}$ and $\psi_{\lambda''}$ is given by

$$
\begin{aligned}
I_1 = {} &\sum_\ell e^{-i\boldsymbol{k}_\mu\cdot\boldsymbol{R}_l}\cos[\boldsymbol{k}_{\lambda'}\cdot(\boldsymbol{R}_l - \boldsymbol{R}_{\lambda'})]e^{-|\boldsymbol{R}_l - \boldsymbol{R}_{\lambda'}|/L_{\lambda'}} \\
&\times \cos[\boldsymbol{k}_{\lambda''}\cdot(\boldsymbol{R}_l - \boldsymbol{R}_{\lambda''})]e^{-|\boldsymbol{R}_l - \boldsymbol{R}_{\lambda''}|/L_{\lambda''}}.
\end{aligned}
\tag{24}
$$

The above sum I_1 can be reduced, by taking the origin of the sum as $\boldsymbol{R}_{\lambda'} = \boldsymbol{0}$ and the nearest-neighbor position from the origin as $\boldsymbol{R}_{\lambda''} = \Delta\boldsymbol{R}_{\lambda''}$, to

$$
I_1 = \sum_\ell f(\boldsymbol{R}_\ell)f(\boldsymbol{R}_\ell - \Delta\boldsymbol{R}_{\lambda''})e^{-i\boldsymbol{k}_\mu\cdot\boldsymbol{R}_\ell},
\tag{25}
$$

where the even function $f(\boldsymbol{X}_\ell)$ is defined as

$$
f(\boldsymbol{X}_\ell) = \cos(\boldsymbol{k}_{\lambda'}\cdot\boldsymbol{X}_\ell)\,e^{-|\boldsymbol{X}_l|/L_{\lambda'}}.
\tag{26}
$$

Since the localization lengths of SL modes are the same, e.g., $L_{\lambda'} \cong L_{\lambda''}$, hereafter we denote this as L. As $f(\boldsymbol{X}_\ell)$ is concerned with SL modes, the relevant sum should be made in the region $|\boldsymbol{X}_\ell| \leqslant L$, so we can approximate the summation by

$$
\begin{aligned}
I_1 \cong {} &\frac{1}{\Omega}\int_{|\boldsymbol{X}_\ell|<L}d\boldsymbol{R}_\ell\, f(\boldsymbol{R}_\ell)f(\boldsymbol{R}_\ell - \Delta\boldsymbol{R}_{\lambda''})e^{-i\boldsymbol{k}_\mu\cdot\boldsymbol{R}_\ell} \\
\cong {} &\frac{1}{\Omega}\int_{|\boldsymbol{X}_\ell|<L}d\boldsymbol{R}_\ell\, e^{\frac{-|\boldsymbol{R}_\ell|-|\boldsymbol{R}_\ell - \Delta\boldsymbol{R}_{\lambda''}|}{L}}e^{-i\boldsymbol{k}_\mu\cdot\boldsymbol{R}_\ell} \\
&\times\bigg[\frac{1}{2}\cos(2\boldsymbol{k}_{\lambda'}\cdot\boldsymbol{R}_\ell - \boldsymbol{k}_{\lambda'}\cdot\Delta\boldsymbol{R}_{\lambda''}) + \frac{1}{2}\cos(\boldsymbol{k}_{\lambda'}\cdot\Delta\boldsymbol{R}_{\lambda''})\bigg] \\
\cong {} &|\Delta\boldsymbol{R}_{\lambda''}|\pi L^2\frac{1}{2\Omega}e^{-|\Delta\boldsymbol{R}_{\lambda''}|/L},
\end{aligned}
\tag{27}
$$

where we have used the approximation $\cos(\boldsymbol{k}_{\lambda'}\cdot\Delta\boldsymbol{R}_{\lambda''}) \approx \cos(k_{\lambda'}nL) \approx 1$ from the Ioffe-Regel condition $L \approx 2\pi/k_{\lambda'}$ for SL modes and $e^{-i\boldsymbol{k}_\mu\cdot\boldsymbol{R}_\ell} \approx 1$ due to $|\boldsymbol{k}_\mu| \ll 2\pi/L$ for the wave number of extended acoustic modes. The term containing $\cos(2\boldsymbol{k}_{\lambda'}\cdot\boldsymbol{R}_\ell - \boldsymbol{k}_{\lambda'}\cdot\Delta\boldsymbol{R}_{\lambda''})$ becomes negligible since it yields a rapidly oscillating function in the integrand.

This gives the squared hopping integral of the form

$$
I_1^2 \simeq \left(\frac{\pi\Delta R_{\lambda''}L^2}{2\Omega}\right)^2 e^{-2\Delta R_{\lambda''}/L},
\tag{28}
$$

where $\Delta R_{\lambda''}$ is the hopping distance.

In the temperature regime $T \simeq$ a few 10 K, i.e., $k_B T > \hbar \omega_{\lambda'}, \hbar \omega_{\lambda''} > \hbar \omega_{\boldsymbol{k}_\mu}$, the inverse of the relaxation time takes the following form under the above conditions and by employing the linear dispersion relation for the extended phonon mode $\omega_{\boldsymbol{k}_\mu} = v_\mu k_\mu$,

$$
\frac{1}{\tau_{\lambda'}^{\text{same}}} \cong \frac{2\pi k_B T (D_r + D_\phi)^2 C I_1^2}{\hbar^3 V L^6 v_\parallel^2}
$$
$$
\times \sum_{\boldsymbol{k}_\parallel, \lambda''} \left[\frac{\delta(\omega_{\lambda''} - \omega_{\lambda'} - \omega_{\boldsymbol{k}_\parallel})}{\omega_{\lambda''}^2} + \frac{\delta(\lambda' \rightleftarrows \lambda'')}{\omega_{\lambda''}^2} \right]
$$
$$
+ [2 \times (D \longrightarrow S, \parallel \longrightarrow \perp) \text{ in the above}]. \quad (29)
$$

Here the coefficient C is defined in Eq. (21). We have omitted the temperature-independent term providing only small contributions.

B. Thermal conductivity due to the hopping of SL modes

In the previous subsection, we have formulated the relaxation rate of SL modes due to the anharmonic interaction between SL modes and extended modes. This is a quantum process realizing the decay of the SL′ mode to the SL″ mode assisted by the extended mode: SL′ + extended → SL″. Without anharmonic interaction, SL modes cannot diffuse/contribute to thermal transport. This means that the plateau region should continue at higher temperatures after its emergence, i.e., the contribution from extended modes to lattice thermal conductivity is saturated at higher temperatures due to the weak localization of acoustic modes, as explained in Sec. II. Thus, the T-linear rise of $\kappa_L(T)$ cannot recover without anharmonic interaction between SL modes and extended modes.

In addition, we emphasize that disorder, induced by off-centeredness as shown in the supplemental material [22], is essential to generate the hopping of SL modes. This occurs only in the case in which the SL′ mode belonging to the eigenfrequency $\omega_{\text{SL}'}$ can hop to a site of the SL″ mode with a different eigenfrequency $\omega_{\text{SL}''}$ via absorption or emission of the extended mode with finite frequency $\pm(\omega_{\text{SL}'} - \omega_{\text{SL}''})$. This finite frequency is created by level repulsion between eigenfrequencies due to disorder, i.e., localized modes never belong to the same eigenfrequency according to the level repulsion.

Let us provide the formula of $\kappa_L(T)$ due to the diffusion process, where SL modes serve as primary heat carriers. In this process, the characteristic length scale should be the hopping distance $\Delta R_{\lambda''}$ from the site of the SL′ mode to that of the SL″ mode, and the characteristic time scale is the relaxation time $\tau_{\lambda'}$ of the SL′ mode. This leads to the following formula of the lattice thermal conductivity due to the hopping process, which was first proposed for fracton excitations by Alexander *et al.* [15],

$$
\kappa_{\text{hop}}(T) = \frac{1}{3V} \sum_{\lambda'} C_{\lambda'}(T) \frac{\Delta R_{\lambda''}^2}{\tau_{\lambda'}}, \quad (30)
$$

where $\Delta R_{\lambda''}^2 / \tau_{\lambda'}$ is the thermal diffusivity of the SL mode λ', and $C_{\lambda'}(T)$ is the specific heat associated with the SL mode λ'. In the high-temperature regime $T \gtrsim$ a few 10 K, the specific heat follows the Dulong-Petit relation of the form $C_{\lambda'}(T) = k_B$ per the mode λ'. Note that $1/\tau_{\lambda'} = 1/\tau_{\lambda'}^{\text{same}} + 1/\tau_{\lambda'}^{\text{dif}}$. We first

calculate the hopping process between the same polarization by

$$
\kappa_{\text{hop}}^{\text{same}}(T) = \frac{k_B}{3V} \sum_{\lambda'} \frac{\Delta R_{\lambda''}^2}{\tau_{\lambda'}^{\text{same}}}. \quad (31)
$$

The substitution of Eq. (29) into Eq. (31) together with Eq. (28) yields

$$
\kappa_{\text{hop}}^{\text{same}}(T) \cong \frac{k_B}{3V^2} \frac{\pi^3 k_B T (D_r + D_\phi)^2 C}{2\hbar^3 v_\parallel^2 L^2 \Omega^2} \sum_{\boldsymbol{k}_\parallel, \lambda', \lambda''} \frac{\Delta R_{\lambda''}^4}{\omega_{\lambda''}^2}
$$
$$
\times e^{-2\Delta R_{\lambda''}/L} [\delta(\omega_{\lambda''} - \omega_{\lambda'} - \omega_{\boldsymbol{k},\parallel}) + \delta(\lambda' \rightleftarrows \lambda'')]
$$
$$
+ [2 \times (D \longrightarrow S, \parallel \longrightarrow \perp) \text{ in the above}]. \quad (32)
$$

Transforming the sum $\sum_{\boldsymbol{k}_\mu}$ for extended phonon modes to the integral $V/(2\pi)^3 \int d\boldsymbol{k}_\mu = V/(2\pi^2 v_\mu^3) \int \omega_{k_\mu}^2 d\omega_{k_\mu}$, we have

$$
\kappa_{\text{hop}}^{\text{same}}(T) = \frac{\pi k_B^2 T C}{12\hbar^3 V \Omega^2 L^2} \left[\frac{(D_r + D_\phi)^2}{v_\parallel^5} + 2\frac{(S_r + S_\phi)^2}{v_\perp^5} \right]
$$
$$
\times \sum_{\lambda'', \lambda'} \Delta R_{\lambda''}^4 e^{-2\Delta R_{\lambda''}/L} \frac{(\omega_{\lambda''} - \omega_{\lambda'})^2}{\omega_{\lambda''}^2}. \quad (33)
$$

The sum on λ' and λ'' above should include the density of states of SL modes $D_{\text{SL}}(\omega_{\lambda'})$ and $D_{\text{SL}}[\omega_{\lambda'}(\Delta R_{\lambda''})]$ for the same polarization process. The volume Ω should contain two independent SL modes corresponding to two independent in-plane mode, say, stretching or libration, in the bandwidth of $\Delta\omega_{\text{sl}}$, which leads to

$$
D_{\text{SL}}(\omega_{\lambda'}) \Omega \Delta\omega_{\text{sl}} = 2 \quad (34)
$$

and

$$
D_{\text{SL}}[\omega_{\lambda''}(\Delta R_{\lambda''})] \Omega \Delta\omega_{\text{sl}} = 1, \quad (35)
$$

where the volume Ω contains at least one possible SL mode λ'' with the same (different) polarization as (from) mode λ'. Since the term $\Delta R_{\lambda''}^4 e^{-2\Delta R_{\lambda''}/L}$ in Eq. (35) achieves its maximum at $\Delta R_{\lambda''} = 2L$ and it decays fast with further increasing of $\Delta R_{\lambda''}$, the sum of λ'' could be estimated within the sphere region $\Delta R_{\lambda''} \leqslant \Delta R$,

$$
\sum_{\lambda'', \lambda'} \Delta R_{\lambda''}^4 e^{-2\Delta R_{\lambda''}/L} \frac{(\omega_{\lambda''} - \omega_{\lambda'})^2}{\omega_{\lambda''}^2}
$$
$$
\cong \frac{\frac{4\pi}{3} \Delta R^3 2V}{\Omega^2} \Delta R^4 e^{-2\Delta R/L} \times (10^{-2}). \quad (36)
$$

Here the sum on SL modes is done by $\sum_{\lambda''} = 4\pi \Delta R^3/3 \int_{\omega_{\text{sl}}}^{\omega_{\text{sl}}+\Delta\omega_{\text{sl}}} D[\omega_{\lambda''}(\Delta R_{\lambda''})] d\omega_{\lambda''}$ and $\sum_{\lambda'} = V \int_{\omega_{\text{sl}}}^{\omega_{\text{sl}}+\Delta\omega_{\text{sl}}} D(\omega_{\lambda'}) d\omega_{\lambda'}$, where the factor $4\pi \Delta R^3/3\Omega$ from Eq. (35) means the total number of hopping sites from λ' to λ'' for the same polarization process, and $2V/\Omega$ from Eq. (34) is the total number of λ' contributing to the thermal conductivity κ_{hop}. The numerical factor 10^{-2} arises from the magnitude estimation of the integral $\int_{\omega_{\text{sl}}}^{\omega_{\text{sl}}+\Delta\omega_{\text{sl}}} d\omega_{\lambda'} \int_{\omega_{\text{sl}}}^{\omega_{\text{sl}}+\Delta\omega_{\text{sl}}} d\omega_{\lambda''} \frac{(\omega_{\lambda''} - \omega_{\lambda'})^2}{\Delta\omega_{\text{sl}}^2 \omega_{\lambda''}^2}$.

The formula of the thermal conductivity due to the hopping mechanism between the same polarization is given by

$$\kappa_{\text{hop}}^{\text{same}}(T) = \frac{\pi^2 k_B^2 T \Delta R^7}{144 \rho m'^2 \Omega^2 L^2} e^{-2\Delta R/L} (10^{-2})$$
$$\times \left[\frac{(D_r + D_\phi)^2}{v_\parallel^5} + 2 \frac{(S_r + S_\phi)^2}{v_\perp^5} \right]. \quad (37)$$

The same procedure for the hopping process due to anharmonic interaction between different polarizations leads to

$$\kappa_{\text{hop}}^{\text{dif}}(T) = \frac{4^2 k_B^2 T \Delta R^7}{144 \rho m'^2 \Omega^2 L^2} e^{-2\Delta R/L} (10^{-2})$$
$$\times \left[\frac{(D_r - D_\phi)^2}{v_\parallel^5} + 2 \frac{(S_r - S_\phi)^2}{v_\perp^5} \right]. \quad (38)$$

The total thermal conductivity due to the hopping mechanism is given by the sum of these components as

$$\kappa_{\text{hop}}(T) = \kappa_{\text{hop}}^{\text{same}}(T) + \kappa_{\text{hop}}^{\text{dif}}(T). \quad (39)$$

C. Evaluation of anharmonic coupling constants D and S

Here we estimate the anharmonic coupling constants $D_{r(\phi)}$ and $S_{r(\phi)}$ by illustrating type-I BGS. The coupling constants $D_r(S_r)$ and $D_\phi(S_\phi)$ are associated with the stretching and libration motion of guest-cage vibrations identified by the force constant ξ_r and ξ_ϕ in Eq. (6) by the relation $\xi_{r(\phi)} = m'\omega_{r(\phi)}^2$, where m' is the reduced mass defined by $1/m' = 1/m + 1/M$. In our coarse-grained Hamiltonian introduced in Sec. III, the guest ion Ba(2) in the tetrakaidecahedron cage has mass m, and the molecular unit composed of 1 tetrakaidecahedron and 1/3 dodecahedron has total mass M excluding the off-center guest ion.

We first evaluate the coupling constants $D_{r(\phi)}$ from the Raman spectroscopy data of the pressure dependence [23]. The D_r can be related to the pressure P by

$$D_r = \frac{\partial \xi_r}{\partial e_{\alpha\alpha}} = 3B \frac{\partial \xi_r}{\partial \omega^r} \frac{\partial \omega^r}{\partial P} = 3B(2m'\omega_0^r) \frac{\partial \omega^r}{\partial P}. \quad (40)$$

Here $B = \frac{\Delta P}{(\Delta V/V)}$ is the bulk modulus, where the dilation is given by $\Delta V/V = \sum_\alpha e_{\alpha\alpha}$ for cubic structure. The coupling constant D_ϕ can be defined in a similar manner to Eq. (40) as

$$D_\phi = \frac{\partial \xi_\phi}{\partial e_{\alpha\alpha}} = 3B(2m'\omega_0^\phi) \frac{\partial \omega^\phi}{\partial P}. \quad (41)$$

In the pressure range from 0.8 to 5.8 GPa, the E_g mode spans from 20 to 27 cm^{-1}, while for T_{2g} mode it ranges from 17 to 27 cm^{-1}. The observed spectra of these two modes are overlapped/mixed, indicating the narrowing of the spectra with increasing pressure. Taking account of these aspects, we have $\partial \omega^r/\partial P = 2\pi \times 4.2 \times 10^{10}$ s^{-1} GPa^{-1} and $\partial \omega^\phi/\partial P = 2\pi \times 6.0 \times 10^{10}$ s^{-1} GPa^{-1}. We then obtain the coupling constants $D_r = m'\pi^2 \times 3.0 \times 10^{25}$ kg s^{-2} and $D_\phi = m'\pi^2 \times 3.0 \times 10^{25}$ kg s^{-2} using the observed bulk modulus $B = 41.3$ GPa [24]. To the best of our knowledge, the experiment data for estimating the coupling coefficients $S_{r(\phi)}$ are not available, so we assume $S_r \approx D_r$ and $S_\phi \approx D_\phi$ at the

present stage. The above coupling constants yield

$$\kappa_{\text{hop}} = 3.3 \times 10^{-3} T \text{ (W m}^{-1} \text{ K}^{-1}), \quad (42)$$

where we have employed the values of parameters in Eq. (39) as the localization length $L = 2a_0$, the hopping distance $\Delta R = 3.5L$, the volume of molecular unit $\Omega = (a_0)^3/6$, the lattice spacing $a_0 = 11.68$ Å, and the mass density $\rho = 6.01 \times 10^3$ kg/m^3, in addition to the velocities of acoustic phonons $v_\parallel = 3369$ m/s and $v_\perp = 1936$ m/s [9]. The value of κ_{hop} in Eq. (42) is smaller than the observed value of $\kappa_{\text{hop}} = 9.2 \times 10^{-3} T$ (W m^{-1} K^{-1}) for type-I BGS. This mainly arises, as will be demonstrated below by means of FPC, from the underestimated shear coupling constants $S_{r(\phi)}$ obtained by assuming the relations $S_{r(\phi)} \approx D_{r(\phi)}$.

Due to the lack of experiment data for the shear coupling coefficients $S_{r(\phi)}$, we have performed FPC for type-I BGS to obtain the coupling constants from the shift of eigenfrequencies at the Γ-point of the low-lying optical mode by imposing strain to the cage structure. The normal strain is isotropic and defined as $e_{\alpha\alpha} = (a_0 - a)/a_0$, where a_0 and a are the lattice constant for the unstrained and strained unit cell [25], respectively. The shear strain is also isotropic and defined as $e_{\alpha\beta} = [1 - \sqrt{1 - (2\cos\theta - 1)\cos\theta}]/(2\cos\theta - 1)$, where θ is the acute angle between edges after deformation.

We have performed the FPC using the VASP code [26] with the Perdew-Burke-Ernzerhof functional and the PAW method [27], the plane-wave cutoff energy 250 eV, and the force convergence less than 10^{-7} eV/Å. The phonon frequencies are calculated using the PHONOPY code [28] with the $4 \times 4 \times 4$ Monkhorst-Pack k grids and for a unit cell containing 54 atoms. The coupling constants obtained from normal strain are $D_r = m'\pi^2 \times 2.1 \times 10^{25}$ kg s^{-2}, $D_\phi = m'\pi^2 \times 1.5 \times 10^{25}$ kg s^{-2}, and from a sheared unit cell they are $S_r = m'\pi^2 \times 4.2 \times 10^{25}$ kg s^{-2}, $S_\phi = m'\pi^2 \times 2.9 \times 10^{25}$ kg s^{-2}, respectively. The $D_{r(\phi)}$ are smaller than those estimated from the Raman spectroscopy data of pressure dependence, though $S_{r(\phi)}$ are larger than the values obtained from the assumption $S_{r(\phi)} \approx D_{r(\phi)}$. The above coupling constants yield the thermal conductivity due to the hopping of SL modes of

$$\kappa_{\text{hop}} = 4.8 \times 10^{-3} T \text{ (W m}^{-1} \text{ K}^{-1}). \quad (43)$$

We remark here that our FPC provides the results for the on-center positioned Ba(2) because the optimization for off-center structure is quite time-consuming and may require us to take into account the dipole-dipole interaction due to off-centeredness and the temperature effect. The on-center structure gives rise to the underestimated coupling constants S since on-center guest ions should respond more weakly to shear distortion than off-center guest ions. Then, the actual $S_{r(\phi)}$ should be larger than the above estimation. Under these situations, the calculated value in Eq. (43) provides sufficient agreement to claim the relevance of the hopping process of SL modes, with the observed $\kappa_{\text{hop}} = \gamma T$ with $\gamma = 9.2 \times 10^{-3}$ W m^{-1} K^{-2} for type-I BGS [9,10] and $\gamma = 9.0 \times 10^{-3}$ W m^{-1} K^{-2} for type-I EGG [8]. For type-I SGG, several different values around $\gamma \sim 8.0 \times 10^{-3}$ W m^{-1} K^{-2} have been reported [4–6,12], indicating that the experimental data of SGG depend on sample qualities according to synthesis methods. In that respect, it has been reported [6] that a

flux-grown sample shows a glasslike plateau, while a zone-melted sample has a crystalline peak.

VI. SUMMARY AND CONCLUSIONS

Off-center type-I clathrates show lattice thermal conductivities κ_L that are almost identical to those of structural glasses [4,5,7,8,10–12]. In addition, off-center type-I clathrates show the excess density of states at THz frequencies manifesting the boson peak that are identical to those of network-forming glasses [9–11]. These indicate that the symmetry-broken guest ions in cages take charge of the emergence of glasslike $\kappa_L(T)$. In structural glasses, many key aspects of a detailed quantitative description are still missing. This is due to the difficulty in identifying relevant entities or elements at the atomic scale caused by their complex microscopic structures.

In Sec. II, we have pointed out that the PR shown in Fig. 2 provides evidence that extended acoustic phonons carrying heat convert to WL modes at ~1.3 meV in off-center BGS. This energy corresponds to the temperature 3.9 K $\approx$ 1.3 meV/$3.84k_B$ from Wien's displacement law, so that this conversion should be associated with the onset of the plateau observed at several K in off-center type-I clathrates [4,5,7–12].

With further increasing temperature, thermal conductivities above a few 10 K show a linear rise in temperature. This is one of the prominent hallmarks of glasslike thermal conductivity since crystals with translational invariance never show these features. Rather, lattice thermal conductivities of crystalline structures decrease with increasing temperature proportional to $\kappa(T) \propto 1/T$ [29].

The theoretical elucidation of the linear rise in temperature "above" the plateau region has been the main subject of the present paper. Our calculated results given in Sec. V, based on the hopping process, show fairly good agreement with observed thermal conductivities. We emphasize in particular that the anharmonic coupling constants obtained from FPC yield a remarkable agreement with the experimental data of $\kappa(T)$ in both the magnitude and the temperature dependence [4,5,7–12]. At much higher temperatures, the T-linear rise in $\kappa(T)$ does not continue, but $\kappa(T)$ saturates above $T \simeq 100$ K [8–10,12]. In this temperature regime, the treatment based on the quantum-mechanical process does not hold because the lifetime of the excited modes becomes much smaller than the inverse of their frequencies, where the guest ions become free from the constraint of atoms constituting cages. This subject will be discussed elsewhere.

In conclusion, the phenomenon of the T-linear rise of $\kappa_L(T)$ above a few 10 K in off-center type-I clathrates has been explained quantitatively by analytic theory on the grounds that off-center clathrates possess definite microscopic structure. Our successful quantitative clarification is due to the fact that the systems are more tractable than network-forming glasses which are difficult to identify relevant constituents at the atomistic level caused by their complex microscopic structures.

[1] G. A. Slack, in *CRC Handbook of Thermoelectrics*, edited by D. M. Rowe (CRC, Boca Raton, FL, 1995), pp. 407–440.

[2] For example, see the review T. Takabatake, K. Suekuni, T. Nakayama, and E. Kaneshita, Rev. Mod. Phys. **86**, 669 (2014), and references therein.

[3] M. Beekman, D. T. Morelli, and G. S. Nolas, Nat. Mater. **14**, 1182 (2015).

[4] G. S. Nolas, J. L. Cohn, G. A. Slack, and S. B. Schujman, Appl. Phys. Lett. **73**, 178 (1998).

[5] J. L. Cohn, G. S. Nolas, V. Fessatidis, T. H. Metcalf, and G. A. Slack, Phys. Rev. Lett. **82**, 779 (1999).

[6] S. Christensen, M. S. Schmokel, K. A. Borup, G. K. H. Madsen, G. J. McIntyre, S. C. Capelli, M. Christensen, and B. B. Iversen, J. Appl. Phys. **119**, 185102 (2016).

[7] S. Paschen, W. Carrillo-Cabrera, A. Bentien, V. H. Tran, M. Baenitz, Y. Grin, and F. Steglich, Phys. Rev. B **64**, 214404 (2001).

[8] B. C. Sales, B. C. Chakoumakos, R. Jin, J. R. Thompson, and D. Mandrus, Phys. Rev. B **63**, 245113 (2001).

[9] M. A. Avila, K. Suekuni, K. Umeo, H. Fukuoka, S. Yamanaka, and T. Takabatake, Phys. Rev. B **74**, 125109 (2006).

[10] M. A. Avila, K. Suekuni, K. Umeo, H. Fukuoka, S. Yamanaka, and T. Takabatake, Appl. Phys. Lett. **92**, 041901 (2008).

[11] K. Suekuni, M. A. Avila, K. Umeo, H. Fukuoka, S. Yamanaka, T. Nakagawa, and T. Takabatake, Phys. Rev. B **77**, 235119 (2008).

[12] K. Suekuni, M. A. Avila, K. Umeo, and T. Takabatake, Phys. Rev. B **75**, 195210 (2007).

[13] See, for example, T. Nakayama, Rep. Prog. Phys. **65**, 1195 (2002).

[14] Y. Liu, Q. Xi, J. Zhou, T. Nakayama, and B. Li, Phys. Rev. B **93**, 214305 (2016).

[15] S. Alexander, O. Entin-Wohlman, and R. Orbach, Phys. Rev. B **34**, 2726 (1986).

[16] M. L. Williams and H. J. Maris, Phys. Rev. B **31**, 4508 (1985); K. Yakubo, T. Nakayama, and H. J. Maris, J. Phys. Soc. Jpn. **60**, 3249 (1991).

[17] See, for example, T. Nakayama and K. Yakubo, Phys. Rep. **349**, 239 (2001).

[18] J. B. Suck, M. Schreiber, and P. Häussler, *Quasicrystals: An Introduction to Structure, Physical Properties and Applications* (Springer, Berlin, 2002), pp. 403.

[19] T. Nakayama, Phys. Rev. Lett. **80**, 1244 (1998); T. Nakayama and N. Sato, J. Phys.: Condens. Matter **10**, L41 (1998).

[20] T. Mori, K. Iwamoto, S. Kushibiki, H. Honda, H. Matsumoto, N. Toyota, M. A. Avila, K. Suekuni, and T. Takabatake, Phys. Rev. Lett. **106**, 015501 (2011).

[21] Y. Takasu, T. Hasegawa, N. Ogita, M. Udagawa, M. A. Avila, K. Suekuni, I. Ishii, T. Suzuki, and T. Takabatake, Phys. Rev. B **74**, 174303 (2006).

[22] See Supplemental Material at http://link.aps.org/supplemental/10.1103/PhysRevB.96.064306 for the relation between off-centeredness and disorder in Eq. (6).

[23] T. Kume, T. Sukemura, S. Nakano, S. Sasaki, K. Suekuni, and T. Takabatake, Photon Factory Activity Report No. 32, 2014, 2015 (retrive from http://pfwww.kek.jp/acr/2014pdf/part_b/pf14b0145.pdf); T. Sukemura, T. Kume, T. Matsuoka, S. Sasaki, T. Onimaru, and T. Takabatake, J. Phys.: Conf. Ser. **500**, 182022 (2014).

[24] I. Ishii, Y. Suetomi, T. K. Fujita, K. Suekuni, T. Tanaka, T. Takabatake, T. Suzuki, and M. A. Avila, Phys. Rev. B **85**, 085101 (2012).

[25] J. Chen, J. H. Walther, and P. Koumoutsakos, Nano Lett. **14**, 819 (2014).

[26] G. Kresse and J. Furthmüller, Phys. Rev. B **54**, 11169 (1996).

[27] J. P. Perdew, K. Burke, and M. Ernzerhof, Phys. Rev. Lett. **77**, 3865 (1996).

[28] A. Togo and I. Tanaka, Scr. Mater. **108**, 1 (2015).

[29] E. M. Lifshitz and L. P. Pitaevskii, in *Physical Kinetics* (Elsevier, Amsterdam, 1979), Chap. 68.